Published in final edited form as:
Clin Cancer Res. 2015 January 1; 21(1): 166–174. doi:10.1158/1078-0432.CCR-14-1385.

Cabozantinib overcomes crizotinib resistance in ROS1 fusion positive cancer

Ryohei Katayama[1], **Yuka Kobayashi**[1,2], **Luc Friboulet**[3,4], **Elizabeth. L. Lockerman**[3,4], **Sumie Koike**[1], **Alice T. Shaw**[3,4], **Jeffrey A. Engelman**[3,4], and **Naoya Fujita**[1,2,†]

[1]Division of Experimental Chemotherapy, Cancer Chemotherapy Center, Japanese Foundation for Cancer Research, Tokyo 135-8550, JAPAN

[2]Department of Medical Genome Science, Graduate School of Frontier Science, The University of Tokyo, Tokyo 108-8639, JAPAN

[3]Massachusetts General Hospital Cancer Center, Boston, MA 02129, USA

[4]Department of Medicine, Harvard Medical School, Boston, MA 02115, USA

Abstract

Purpose—*ROS1* rearrangement leads to constitutive ROS1 activation with potent transforming activity. In an ongoing phase 1 trial, the ALK tyrosine kinase inhibitor (TKI) crizotinib shows remarkable initial responses in patients with non-small cell lung cancer (NSCLC) harboring *ROS1* fusions; however, cancers eventually develop crizotinib resistance due to acquired mutations such as G2032R in ROS1. Thus, understanding the crizotinib resistance mechanisms in *ROS1* rearranged NSCLC and identification of therapeutic strategies to overcome the resistance are required.

Experimental Design—The sensitivity of CD74-ROS1-transformed Ba/F3 cells to multiple ALK inhibitors was examined. Acquired ROS1 inhibitor resistant mutations in CD74-ROS1 fusion were screened by N-ethyl-N-nitrosourea mutagenesis with Ba/F3 cells. To overcome the resistance mutation, we performed high throughput drug screening with small molecular inhibitors and anticancer drugs used in clinical practice or being currently tested in clinical trials. The effect of the identified drug was assessed in the CD74-ROS1 mutant Ba/F3 cells and crizotinib resistant patient-derived cancer cells (MGH047) harboring G2032R mutated CD74-ROS1.

Results—We identified multiple novel crizotinib resistance mutations in the ROS1 kinase domain including the G2032R mutation. As the result of high-throughput drug screening, we found that the cMET/RET/VEGFR inhibitor cabozantinib (XL184) effectively inhibited the survival of CD74-ROS1-WT and resistant mutants harboring Ba/F3 and MGH047 cells. Furthermore, cabozantinib could overcome all the resistance by all newly identified secondary mutations.

†Corresponding author: Naoya Fujita, Cancer Chemotherapy Center, Japanese Foundation for Cancer Research, 3-8-31, Ariake, Koto-ku, Tokyo 135-8550, JAPAN, Phone: +81-3-3520-0111; Fax: +81-3-3570-0484; naoya.fujita@jfcr.or.jp.

Conclusions—We developed a comprehensive model of acquired resistance to ROS1 inhibitors in NSCLC with *ROS1* rearrangement and identified cabozantinib as a therapeutic strategy to overcome the resistance.

Keywords

ROS1 rearrangement; resistance; crizotinib; cabozantinib; mutagenesis

INTRODUCTION

An increasing number of genetic alterations that aberrantly activate tyrosine kinases have been identified as oncogenic drivers of non-small cell lung cancer (NSCLC). Active mutations of epidermal growth factor receptor (EGFR), such as the L858R point mutation or deletion/insertion of several amino acids between exons 19 and 20, are more commonly observed in NSCLC patients. The active mutation of KRAS is also predominantly found in NSCLC patients. In addition to these active oncogene mutations, chromosomal rearrangements involving the tyrosine kinase domains of *ALK*, *ROS1*, and *RET* are observed in 1%–5% of NSCLC patients (1). The oncogenic fusion protein in NSCLC can be targeted by tyrosine kinase inhibitors such as crizotinib; therefore, a number of specific tyrosine kinase inhibitors targeting the fusion tyrosine kinase are currently under development. Although EGFR inhibitors (e.g., gefitinib or erlotinib) or the ALK inhibitor crizotinib show remarkable efficacy in most cases, the majority of patients will develop tumors resistant to targeted therapies in less than 1 year of treatment (2, 3). In cancers harboring the ALK fusion protein, several mechanisms of crizotinib resistance have been reported, including acquired secondary mutations in the kinase domain of ALK, genomic amplification of the *ALK* fusion gene, and amplification or activation of other kinases (3–7).

Recently, crizotinib was shown to be an effective inhibitor of ROS1 tyrosine kinase, and two case reports have described the activity of crizotinib in patients with *ROS1*-rearranged lung cancers (8, 9). Although crizotinib exhibited activity in an NSCLC patient harboring the *ROS1* fusion, a resistant tumor eventually emerged. Recently, the G2032R mutation in the ROS1 kinase domain was identified in a crizotinib-treated resistant tumor, which was not observed before treatment (10). The mutation was located in the solvent-front region of the ROS1 kinase domain and was analogous to the G1202R ALK mutation identified in crizotinib-resistant ALK-rearranged lung cancers. We previously reported that the ALK G1202R mutation confers high-level resistance to crizotinib compared with all next-generation ALK inhibitors that were examined (3). Therefore, it is important to identify novel compounds that can overcome the G2032R ROS1 mutation, which confers crizotinib resistance in these cancers.

In this study, we tested several ALK inhibitors to examine the potency of the sterically distinct ALK inhibitors, because the kinase domains of ALK and ROS1 are highly similar and grouped in the same kinase family (11). Subsequently, we identified a number of different crizotinib and/or ceritinib resistant mutations including G2032R mutation in the ROS1 kinase domain by N-ethyl-N-nitrosourea (ENU)-driven accelerated mutagenesis screening. High throughput inhibitor screening identified several kinase inhibitors as a

potent ROS1 inhibitor, and identified that the cMET/RET/vascular endothelial growth factor (VEGFR) inhibitor cabozantinib can potently inhibit both wild-type (WT) and the resistant mutant CD74-ROS1. On the basis of these results, we propose the use of several inhibitors as alternative therapeutic strategies for ROS1-rearranged cancers and cabozantinib as a key drug for overcoming crizotinib resistance in ROS1 fusion-positive cancer cells lines, particularly those mediated by secondary mutations.

Materials and Methods

Reagents

Crizotinib was obtained from ShangHai Biochempartner (ShangHai, China); alectinib, cabozantinib, and ceritinib (LDK378) were purchased from ActiveBiochem (Hong Kong), 17-AAG was purchased from LC Laboratories (Woburn, MA, USA); NVP-TAE-684 and ASP3026 were purchased from ChemieTek (Indianapolis, IN, USA); AP26113 was purchased from Selleck (Cambridge, MA); and Foretinib was purchased from AdooQ BioScience (Irvine, CA, USA). Each compound was dissolved in dimethyl sulfoxide (DMSO) for cell culture experiments. For inhibitor screening, the SCADS Inhibitor kit was provided by the Screening Committee of Anticancer Drugs supported by a Grant-in-Aid for Scientific Research on Innovative Areas, Scientific Support Programs for Cancer Research, from the Ministry of Education, Culture, Sports, Science, and Technology of Japan.

Isolation of genomic DNA, preparation of total RNA, and sequencing of the *ROS1* fusion gene

Genomic DNA was isolated from cell pellets after proteinase K treatment. The ROS1 kinase domain was amplified by polymerase chain reaction (PCR) from the genomic DNA and sequenced bidirectionally using Sanger sequencing.

Cell culture conditions

Human embryonic kidney 293FT cells (Invitrogen) were cultured in Dulbecco's modified Eagle medium supplemented with 10% fetal bovine serum (D-10). Ba/F3 cells, which are immortalized murine bone marrow-derived pro-B cells, were cultured in D-10 media with or without 0.5 ng/mL of interleukin (IL)-3 (Invitrogen). Crizotinib-resistant ROS1 fusion-positive NSCLC patient-derived MGH047 cells were cultured in ACL-4 medium supplemented with 3% fetal bovine serum (10).

Survival assays

To assess 72-h drug treatment, 2000–3000 cells were plated in replicates of three to six in 96-well plates. Following drug treatments, the cells were incubated with the CellTiter-Glo assay reagent (Promega) for 10 min. Luminescence was measured using a Centro LB 960 microplate luminometer (Berthold Technologies). The data were graphically displayed using GraphPad Prism version 5.0 (GraphPad Software). IC_{50} values were determined using a nonlinear regression model with a sigmoidal dose response in GraphPad.

Immunoblot analysis

Lysates were prepared as previously described (3, 12). Equal volumes of lysate were electrophoresed and immunoblotted with antibodies against phospho-ROS1 (Tyr2274), ROS1 (69D6), phospho-p42/44 ERK/MAPK (Thr202/Tyr204), p42/44 ERK/MAPK, phospho-Akt (Ser473) (D9E), panAkt (C67E7), phospho-S6 ribosomal protein (Ser240/244, D68F8), S6 ribosomal protein (54D2), STAT3 (79D7), phospho-STAT3 (Tyr705) (Cell Signaling Technology), GAPDH (6C5, Millipore), and β-actin (Sigma).

Retroviral infection

cDNA encoding WT or mutant CD74-ROS1 was cloned into 1520 retroviral expression vectors (pLenti), and viruses were replicated in 293FT cells by transfecting with packaging plasmids. After retroviral infection, Ba/F3 cells were selected by incubation with puromycin (0.7 μg/mL) for two weeks. For Ba/F3 cells infected by CD74-ROS1 variants, IL-3 was withdrawn from the culture medium at least two weeks before the experiments.

ENU mutagenesis screening

The ENU mutagenesis screening protocol was based on procedures published by Bradeen et al. (13, 14) and O'Hare et al. (14). Briefly, ENU (Sigma) was dissolved in DMSO at a concentration of 100 mg/mL. All materials that came in contact with ENU were decontaminated with 0.2 M NaOH. For each resistance screen, approximately 1.5×10^8 Ba/F3 CD74-ROS1 cells in a total of 160 mL of growth media were exposed to a final concentration of 100 mg/mL of ENU. After approximately 16 h, the cells were collected by centrifugation, washed, and incubated for 24 h. After a 24-h recovery period, the cells were split into five aliquots of 3×10^7 cells each. Crizotinib or ceritinib was added at a final concentration of 30, 50, 100, or 200 nM, and cells of each aliquot were distributed into five 96-well plates (5×10^4 cells in 100 μL media per well). Plates were incubated over a course of four weeks with regular inspection. When clear signs of cell growth were microscopically observed and a color change of the media occurred, the content of the respective well was transferred into 1 mL of growth media containing the original concentration of MET inhibitor in a 24-well plate. After approximately one week of expansion, the cell number was sufficient for further processing (see below).

Identification of ROS1 mutations

Genomic DNA was prepared by lysing the cells with proteinase K buffer, which was heat inactivated at 95°C for 5 min. Then, the temperature was gradually decreased by 2°C/min. For sequence analysis, a DNA fragment covering the entire kinase domain of ROS1 was amplified using KOD Plus (TOYOBO). The PCR products were then purified with a gel purification kit (GE healthcare) and sequenced using standard Sanger sequencing.

Drug screening

Inhibitor screening was conducted using a subset of the modified SCADS library containing 282 compounds in three 96-well microplates. Parental, CD74-ROS1-WT- or CD74-ROS1-G2032R-expressing Ba/F3 cells were seeded in triplicates in 96-well plates on day 1, and each inhibitor was added at 10 nM, 100 nM, 1 μM, and 3 μM on the same day. Cell viability

was determined on day 4 using the CelTiter Glo assay. The cell viability from triplicate plates were averaged to determine relative cell growth compared with that of DMSO-treated controls.

Statistical analysis

All data are presented as means ± SD. Statistical analysis was performed using the two-tailed Student's *t*-test. Significance was established for p values <0.05.

RESULTS

Several ALK inhibitors effectively inhibit CD74-ROS1 fusion

The tyrosine kinase domains of ALK and ROS1 shared 70% identity, and both kinases belong to the same branch in a kinase phylogenic tree (11). To identify inhibitors capable of inhibiting the kinase activities of the ROS1 fusion protein, we tested the potency of various ALK inhibitors to CD74-ROS1. First, we established IL-3 independently growing Ba/F3 cells by transformation with *CD74-ROS1*, which is the most frequently observed *ROS1* fusion gene in NSCLC. From the polyclonal CD74-ROS1-addicted Ba/F3 cells, we picked up the clone with a high expression of CD74-ROS1 and similar crizotinib sensitivity to the polyclonal cells (clone #6, Supplementary Figure S1), which was propagated to examine the sensitivity to various ALK inhibitors currently being clinically evaluated. Our results showed that crizotinib, ceritinib (LDK378), and AP26113 exhibited remarkable growth suppression of CD74-ROS1 Ba/F3 cells, ASP3026 showed moderate inhibitory activity, and alectinib (CH5424802) showed none (Figures 1A and 1B). Corresponding to the cell growth inhibiting activity, crizotinib, ceritinib, AP26113 and ASP3026, but not alectinib inhibited phospho-ROS1 and its downstream phospho-STAT3 in a dose-dependent manner (Figure 1C). Among these compounds, crizotinib and ceritinib are clinically available for ALK fusion-positive NSCLC. Furthermore, ceritinib, AP26113, and ASP3026 were shown to be active against the ALK gatekeeper mutation (L1196M), which is most frequently observed in crizotinib-resistant ALK-rearranged NSCLC (15). Therefore, we decided to identify potential resistance mechanisms to crizotinib or ceritinib in CD74-ROS1 mediated by a resistance mutation in the ROS1 kinase domain.

Identification of crizotinib- and ceritinib-resistant Ba/F3 CD74-ROS1 cells by accelerated mutagenesis screening

To identify *ROS1* mutations responsible for resistance to crizotinib or ceritinib in ROS1 fusion-positive cancers, we performed random mutagenesis screening by exposing the CD74-ROS1 Ba/F3 cells to the alkylating agent ENU, followed by selection using various concentration of crizotinib or ceritinib. After culturing with the inhibitors for 3–4 weeks, we observed an inhibitor dose-dependent reduction in the number of wells with growing cells. The resistant cells were recovered and the ROS1 kinase domains were sequenced. The resistant clones were selected by treatment with 200 nM of crizotinib or ceritinib, and all carried the G2032R mutation (Figure 2A). Of the clones selected with 100 nM crizotinib, one clone harbored the K2003I mutation in the CD74-ROS1 and a second clone harbored no mutation. After expanding the isolated clone from ENU mutagenesis screening harboring K2003I mutated CD74-ROS1, we tested the sensitivity to crizotinib and ceritinib. We found

that K2003I-mutated ROS1 did not confer resistance to crizotinib or ceritinib. On the other hand, G2032R-mutated CD74-ROS1 conferred high resistance to both crizotinib and ceritinib (Figures 2B and 2C). When the cells were selected using a lower concentration of crizotinib (50 nM) or ceritinib (100 nM), various mutations in the clones were identified (Supplementary Figure S2). Next, we tested the isolated clones from ENU mutagenesis for crizotinib or ceritinib sensitivity. The recovered Ba/F3 cells harboring the mutations E1990G with M2128V, L1951R, G2032R, or L2026M with K2003I in ROS1 showed IC_{50} values against crizotinib that were more than 3-fold higher than that of WT CD74-ROS1 expressing BaF3 cells (Supplementary Figures S3A and S3B). On the other hand, Ba/F3 CD74-ROS1 cells harboring the L2026M mutation, which is a gatekeeper mutation corresponding to L1196M in ALK, were sensitive to ceritinib. Likewise, the mutations E1990G with M2128V, L1951R, or G2032R conferred resistance to ceritinib. In particular, the CD74-ROS1 expressing Ba/F3 cells harboring the G2032R mutation were extremely resistant to both crizotinib and ceritinib. Then, we conducted immunoblot analysis of the recovered Ba/F3 cells by treating the cells with various concentrations of crizotinib or ceritinib. The results were consistent with those of the cell viability assay, in which phosphorylation of CD74-ROS1 harboring the G2032R mutation was not completely attenuated even following treatment with 1 μM of crizotinib or ceritinib (Figure 2B). The G2032R mutation was recently identified in a patient with crizotinib refractory CD74-ROS1 fusion-positive NSCLC (10). In contrast, cells carrying the L1951R and E1990G with M2128V mutations exhibited resistance to crizotinib or ceritinib, consistent with the results of the cell viability assay. Cells harboring the L2026M/K2003I double mutant exhibited resistance to crizotinib but not to ceritinib (Supplementary Figure S3C).

To confirm whether these mutations confer resistance to crizotinib and ceritinib, we introduced each mutated CD74-ROS1 in Ba/F3 cells. All of the resistant mutated CD74-ROS1 (L1951R, L1982F, E1990G, F1994L, K2003I, L2026M, and G2032R) maintained transforming activity. Then, we tested the sensitivity of Ba/F3 cells expressing CD74-ROS1 mutants to crizotinib or ceritinib. Similar to the result of the recovered Ba/F3 cells from ENU mutagenesis screening, L1951R and G2032R mutated CD74-ROS1-induced Ba/F3 showed marked resistance to both crizotinib, ceritinib and AP26113. L2026M mutant-induced Ba/F3 cells were resistant to crizotinib but not to ceritinib or AP26113. L1982F, E1990G, or F1994L mutants showed slight resistance to crizotinib and ceritinib. (Figures 3A–C, Supplementary Figures S4A–C).

Next, we mapped these mutations on the crystal structure data of crizotinib: ROS1 to elucidate the location of mutations that confer resistance (Figure 3D and Supplementary Figure S5). L1951 and G2032 mutations were located in the solvent-front region (entrance of the crizotinib binding pocket), and L2026, which correspond to the L1196 mutation in ALK, is a gatekeeper mutation of *ROS1*. All of the identified mutations that conferred higher crizotinib resistance were located close to the crizotinib binding domain of the ROS1 kinase (Figure 3D).

High throughput inhibitor screening identified cabozantinib (XL-184) as a potent ROS1 inhibitor

To identify potent ROS1 kinase inhibitors that selectively suppress the growth of Ba/F3 cells expressing either WT or the crizotinib-resistance mutant CD74-ROS1, we performed cell-based high throughput screening with a series of kinase inhibitors and anticancer agents used in clinical practice or under current clinical evaluation. IL-3-dependent Ba/F3 cells expressing either WT or G2032R-mutated CD74-ROS1 were treated for 72 h with serial dilutions of 282 kinase inhibitors and anticancer drugs in the SCAD inhibitor library. Potential ROS1 kinase inhibitors were selected for further evaluation using the following criteria: selective growth inhibitory effect (<40% cell viability) against WT or G2032R mutated Ba/F3 CD74-ROS1 cells at an inhibitor concentration of ≤100 nM and ≥10-fold lower IC_{50} value compared with that for Ba/F3 parental cells. Using this assay, we newly demonstrated that cabozantinib (XL184), foretinib, TAE684, SB218078, and CEP701, in addition to the ALK inhibitors under clinical evaluation or in clinic, are potent inhibitors of CD74-ROS1 Ba/F3 cell growth (Table 1, Figures 4A, 4B and Supplementary Table S1). Furthermore, among these inhibitors, cabozantinib (XL184), foretinib, and TAE684 effectively inhibited the growth of both WT and G2032R mutated CD74-ROS1 Ba/F3 cells, and the autophosphorylation of both WT and CD74-ROS1 (Figure 4B). Of note, CEP701 showed intermediate selectivity to the growth of CD74-ROS1 Ba/F3 cells, and CEP701 only inhibited the autophosphorylation of WT CD74-ROS1 but not the autophosphorylation of G2032R-mutated CD74-ROS1. And to inhibit the phospho-ROS1 of G2032R mutated CD74-ROS1, higher concentration of TAE684, foretinib or cabozantinib, compared with that for CD74-ROS1 (WT) expressing Ba/F3 cells was needed (Figures 4A and 4B).

Cabozantinib overcomes the crizotinib-resistant CD74-ROS1 mutation

To examine the effect of cabozantinib on cells harboring these mutations, each of the Ba/F3 cells harboring the various CD74-ROS1 mutations (both ENU recovered Ba/F3 clones and CD74-ROS1 mutants transformed Ba/F3 cells) were treated with cabozantinib, and the cell growth and phosphorylation of ROS1 was examined. The results showed that cabozantinib dose-dependently inhibited phospho-ROS1 in all crizotinib-resistant mutant strains and inhibited the growth of all Ba/F3 cells harboring crizotinib-resistant CD74-ROS1 mutations. IC_{50} values of all crizotinib-resistant mutants against cabozantinib were less than 25 nM, although the IC_{50} values of crizotinib resistant mutant (G2032R and L1951R) Ba/F3 cells were approximately 5 to 10 fold higher than that of wildtype CD74-ROS1 harboring Ba/F3 cells (Figure 5 and Supplementary Figures S6 and S7).

In our previous study of clinical crizotinib resistance in ROS1-rearranged NSCLC, we established the MGH047 cell line harboring the CD74-ROS1 G2032R mutation directly isolated from the pleural effusion of a crizotinib-resistant patient. Using this cell line, we compared the activities of cabozantinib and crizotinib and found that crizotinib did not inhibit the growth of MGH047 cells harboring the G2032R mutation, whereas cabozantinib potently inhibited the growth of MGH047 cells (Figure 6A). Furthermore, as exhibited by the Ba/F3 cell line models, cabozantinib effectively suppressed phospho-ROS1 and downstream phospho-Akt, phospho-ERK, and phospho-ribosomal S6 proteins in MGH047 cells (Figure 6B). These results suggest that cabozantinib presents an alternative therapeutic

strategy to treat ROS1-rearranged NSCLC in both crizotinib naïve patients and resistant cases caused by resistance mutations in the kinase domain.

DISCUSSION

Recently, the cMET/ALK/ROS1 inhibitor crizotinib has been clinically evaluated for treatment of ROS1-rearranged NSCLC and has shown remarkable activity (8, 9). Because of the similarity between ROS1 and ALK kinase domains, we examined the sensitivity of various ALK inhibitors on CD74-ROS1 fusion and found that all the tested ALK inhibitors, except for alectinib, effectively inhibited ROS1 fusion. Among those ALK inhibitors, ceritinib was recently approved by the US FDA for ALK-positive patients with crizotinib-resistant or crizotinib-intolerant disease, since high response rate in crizotinib-resistant disease was observed in phase I study (16). Ceritinib has also been shown to be active in both WT and gatekeeper-mutated ALK (L1196M), which causes crizotinib resistance (17). In *EGFR* mutant-positive lung cancers that become resistant to EGFR tyrosine kinase inhibitors, the secondary T790M gatekeeper mutation is detected in roughly one-half of all cases (2). In contrast, in crizotinib-resistant ALK-positive lung cancers, many types of resistance mutations in the ALK kinase domain were identified in various cell lines as well as crizotinib-resistant patients (3). Because the tyrosine kinase domains of ALK and ROS1 share approximately 70% homology, it is possible that many kinds of crizotinib resistance mutations will also occur in ROS1-rearranged NSCLC.

To prospectively identify resistance mutations affecting the ALK/ROS1 inhibitors crizotinib and ceritinib, we performed a cellular drug resistance screen in CD74-ROS1-transformed Ba/F3 cells and identified several resistant mutations, including G2032R, as the most pronounced mutations that confer crizotinib resistance. So far, only the G2032R mutation in *ROS1* has been identified in crizotinib-treated resistant patients with *ROS1*-rearranged NSCLC (10). In this study, the newly identified resistance mutations of L1982F, E1990G, F1994L, and L2026M were less frequent and conveyed milder resistance to crizotinib. In addition, a screen with the structurally distinct ALK/ROS1 inhibitor ceritinib revealed a slightly different mutation profile; however, the most pronounced resistant mutations were L1951R and G2032R. In addition to ENU-induced accelerated mutagenesis screening, we also performed saturated mutagenesis screening (18–20) and identified different unique mutations (E2020K and P2021L), but no G2032R mutation was observed (data not shown). Similarly, a previous study using the same methods to identify crizotinib resistance mutations in EML4-ALK identified unique mutations but did not recapitulate the clinically relevant mutations. These results suggest that induced mutation profiles in mismatch repair-deficient *Escherichia coli* strains might be slightly different from plausible mutations in mammalian cells. However, the mutagenesis screening study with imatinib in Ba/F3 cells harboring BCR-ABL fusion showed that the saturated screening assay is useful to identify various resistance mutations including those with clinical relevance (18).

The mutations identified from ENU accelerated mutagenesis screening can be categorized into three types. The first type includes solvent-front mutations (e.g., L1951R and G2032R), which are located in the solvent-front region of the kinase domain adjacent to the crizotinib-binding site. An amino acid change of the conserved glycine to arginine at position 2032 or

leucine to arginine at position 1951 of the ROS1 kinase domain confers considerable resistance to multiple ALK/ROS1 kinase inhibitors, such as crizotinib, ceritinib, and AP26113. The G2032R ROS1 mutation is analogous to the G1202R *ALK* mutation, which has been identified in *ALK*-rearranged lung cancers that have become resistant to crizotinib, alectinib, and ASP3026 (3). It is likely that these solvent-front mutations decrease the affinity of the mutant ROS1 for crizotinib because of steric hindrance.

The second type includes the gatekeeper mutation L2026M, which is equivalent to gatekeeper mutations observed in EGFR (T790M), ALK fusion (L1196M), and BCR-ABL (T315I). The third type is characterized by helix αC (L1982F or V), which is a homologous residue of L1152 in ALK, previously identified in crizotinib-treated ALK-positive NSCLC patients.

To overcome resistance to crizotinib and ceritinib caused by the G2032R ROS1 mutation, we performed high throughput drug screening, which subsequently identified cabozantinib (XL-184) as a potent ROS1 inhibitor that effectively inhibited both the WT CD74-ROS1 kinase as well as those harboring resistance mutations including G2032R. Furthermore, cabozantinib effectively inhibited the growth of the crizotinib-resistant patient-derived MGH047 cells harboring G2032R mutated CD74-ROS1. Cabozantinib is a small molecule that inhibits the activity of multiple tyrosine kinases, including RET, MET, and VEGFR2. Currently, cabozantinib is clinically available for treatment of refractory medullary thyroid cancer. Data from previous clinical trials revealed a peak plasma concentration of cabozantinib after repeated oral administration (175 mg) of around 1410 ng/mL (2810 nM). Even in the much lower dose (0.64 mg/kg, which is corresponding to about 40 mg oral administration) treated patient, an average peak plasma concentration of cabozantinib after repeated oral administration was around 322 ng/mL (643 nM)(21). Based on the data from our study, we found that cabozantinib at concentrations less than 30 nM inhibited all of the identified crizotinib-resistance mutations, which was much lower than clinically achievable levels. During the preparation of this manuscript, Davare et al. identified that foretinib, which is an oral multi-kinase inhibitor targeting MET, VEGFR-2, RON, KIT, and AXL kinases and currently being clinically evaluated, is a potent inhibitor against ROS1 and overcomes resistance mutations including G2032R (22). Although we confirmed that foretinib also inhibited WT and all mutated crizotinib-resistance ROS1 fusions, our results suggest that cabozantinib is slightly more potent than foretinib. Furthermore, previously reported mean plasma concentrations of foretinib in two clinical trials were 72 nM and 340 nM (23, 24). Although it is impossible to simply compare the plasma concentrations and expected efficacy in humans, cabozantinib is likely to be more potent and effective than foretinib.

In conclusion, our study clearly demonstrated that patients with crizotinib-resistant cancers due to an acquired mutation, such as G2032R, may benefit from more potent and effective ROS1 TKI mutant forms resistant to cabozantinib. Notably, although solvent-front mutations are occasionally observed in crizotinib-resistant ALK fusion-positive NSCLC patients, the frequency of G2032R mutations in ROS1-positive NSCLC has yet to be established. Because secondary mutations, such as the gatekeeper mutation, may not represent the predominant mechanism of acquired crizotinib resistance, additional studies

are needed to elucidate other mechanisms of resistance. The results of these studies will be critical to selecting the best therapeutic strategies for targeting TKI resistance in clinical practice. Although, crizotinib is currently a key agent used to treat cancers harboring *ROS1* translocations, cabozantinib may be able to prevent or overcome resistance to ROS1 inhibitors.

Supplementary Material

Refer to Web version on PubMed Central for supplementary material.

Acknowledgments

We thank Dr. Mark M. Awad at MGH for helping with the establishment of MGH047 cells and Ms. Sidra Mahmood at MGH for helping with the cell survival assay experiments of MGH047 cells. The study was supported in part by JSPS KAKENHI grant number 24300344 and 22112008 (to N. Fujita) and 25710015 (to R. Katayama) and by a research grant from the Princess Takamatsu Cancer Research Fund (to N. Fujita).

References

1. Takeuchi K, Soda M, Togashi Y, Suzuki R, Sakata S, Hatano S, et al. RET, ROS1 and ALK fusions in lung cancer. Nat Med. 2012; 18:378–81. [PubMed: 22327623]
2. Sequist LV, Waltman BA, Dias-Santagata D, Digumarthy S, Turke AB, Fidias P, et al. Genotypic and histological evolution of lung cancers acquiring resistance to EGFR inhibitors. Sci Transl Med. 2011; 3:75ra26.
3. Katayama R, Shaw AT, Khan TM, Mino-Kenudson M, Solomon BJ, Halmos B, et al. Mechanisms of acquired crizotinib resistance in ALK-rearranged lung Cancers. Sci Transl Med. 2012; 4:120ra17.
4. Choi YL, Soda M, Yamashita Y, Ueno T, Takashima J, Nakajima T, et al. EML4-ALK mutations in lung cancer that confer resistance to ALK inhibitors. N Engl J Med. 2010; 363:1734–9. [PubMed: 20979473]
5. Doebele RC, Pilling AB, Aisner DL, Kutateladze TG, Le AT, Weickhardt AJ, et al. Mechanisms of resistance to crizotinib in patients with ALK gene rearranged non-small cell lung cancer. Clin Cancer Res. 2012; 18:1472–82. [PubMed: 22235099]
6. Sasaki T, Koivunen J, Ogino A, Yanagita M, Nikiforow S, Zheng W, et al. A novel ALK secondary mutation and EGFR signaling cause resistance to ALK kinase inhibitors. Cancer Res. 2011; 71:6051–60. [PubMed: 21791641]
7. Sasaki T, Okuda K, Zheng W, Butrynski J, Capelletti M, Wang L, et al. The neuroblastoma associated F1174L ALK mutation causes resistance to an ALK kinase inhibitor in ALK translocated cancers. Cancer Res. 2010
8. Bergethon K, Shaw AT, Ou SH, Katayama R, Lovly CM, McDonald NT, et al. ROS1 rearrangements define a unique molecular class of lung cancers. J Clin Oncol. 2012; 30:863–70. [PubMed: 22215748]
9. Shaw AT, Camidge DR, Engelman JA. Clinical activity of crizotinib in advanced non-small cell lung cancer (NSCLC) harboring ROS1 gene rearrangement. Journal of Clinical Oncology. 2012; 30:abstr 7508.
10. Awad MM, Katayama R, McTigue M, Liu W, Deng YL, Brooun A, et al. Acquired resistance to crizotinib from a mutation in CD74-ROS1. N Engl J Med. 2013; 368:2395–401. [PubMed: 23724914]
11. Manning G, Whyte DB, Martinez R, Hunter T, Sudarsanam S. The protein kinase complement of the human genome. Science. 2002; 298:1912–34. [PubMed: 12471243]
12. Engelman JA, Zejnullahu K, Mitsudomi T, Song Y, Hyland C, Park JO, et al. MET amplification leads to gefitinib resistance in lung cancer by activating ERBB3 signaling. Science. 2007; 316:1039–43. [PubMed: 17463250]

13. Bradeen HA, Eide CA, O'Hare T, Johnson KJ, Willis SG, Lee FY, et al. Comparison of imatinib mesylate, dasatinib (BMS-354825), and nilotinib (AMN107) in an N-ethyl-N-nitrosourea (ENU)-based mutagenesis screen: high efficacy of drug combinations. Blood. 2006; 108:2332–8. [PubMed: 16772610]

14. O'Hare T, Eide CA, Tyner JW, Corbin AS, Wong MJ, Buchanan S, et al. SGX393 inhibits the CML mutant Bcr-AblT315I and preempts in vitro resistance when combined with nilotinib or dasatinib. Proc Natl Acad Sci U S A. 2008; 105:5507–12. [PubMed: 18367669]

15. Lovly CM, Pao W. Escaping ALK inhibition: mechanisms of and strategies to overcome resistance. Sci Transl Med. 2012; 4:120ps2.

16. Shaw AT, Kim DW, Mehra R, Tan DS, Felip E, Chow LQ, et al. Ceritinib in ALK-rearranged non-small-cell lung cancer. N Engl J Med. 2014; 370:1189–97. [PubMed: 24670165]

17. Friboulet L, Li N, Katayama R, Lee CC, Gainor JF, Crystal AS, et al. The ALK Inhibitor Ceritinib Overcomes Crizotinib Resistance in Non-Small Cell Lung Cancer. Cancer Discov. 2014

18. Azam M, Latek RR, Daley GQ. Mechanisms of autoinhibition and STI-571/imatinib resistance revealed by mutagenesis of BCR-ABL. Cell. 2003; 112:831–43. [PubMed: 12654249]

19. Emery CM, Vijayendran KG, Zipser MC, Sawyer AM, Niu L, Kim JJ, et al. MEK1 mutations confer resistance to MEK and B-RAF inhibition. Proc Natl Acad Sci U S A. 2009; 106:20411–6. [PubMed: 19915144]

20. Heuckmann JM, Holzel M, Sos ML, Heynck S, Balke-Want H, Koker M, et al. ALK mutations conferring differential resistance to structurally diverse ALK inhibitors. Clin Cancer Res. 2011; 17:7394–401. [PubMed: 21948233]

21. Kurzrock R, Sherman SI, Ball DW, Forastiere AA, Cohen RB, Mehra R, et al. Activity of XL184 (Cabozantinib), an oral tyrosine kinase inhibitor, in patients with medullary thyroid cancer. J Clin Oncol. 2011; 29:2660–6. [PubMed: 21606412]

22. Davare MA, Saborowski A, Eide CA, Tognon C, Smith RL, Elferich J, et al. Foretinib is a potent inhibitor of oncogenic ROS1 fusion proteins. Proc Natl Acad Sci U S A. 2013; 110:19519–24. [PubMed: 24218589]

23. Eder JP, Shapiro GI, Appleman LJ, Zhu AX, Miles D, Keer H, et al. A phase I study of foretinib, a multi-targeted inhibitor of c-Met and vascular endothelial growth factor receptor 2. Clin Cancer Res. 2010; 16:3507–16. [PubMed: 20472683]

24. Shapiro GI, McCallum S, Adams LM, Sherman L, Weller S, Swann S, et al. A Phase 1 dose-escalation study of the safety and pharmacokinetics of once-daily oral foretinib, a multi-kinase inhibitor, in patients with solid tumors. Invest New Drugs. 2013; 31:742–50. [PubMed: 23054208]

Statement of translational relevance

ROS1 gene rearrangement leads to constitutive ROS1 activation with potent transforming activity. Although crizotinib shows remarkable initial responses, cancers eventually develop resistance to crizotinib. To identify further mechanisms of resistance to crizotinib, we performed ENU mutagenesis screening using CD74-ROS1-expressing Ba/F3 cells, and identified several novel crizotinib resistance mutations in the ROS1 kinase domain including the G2032R mutation, which is observed in the crizotinib resistant patient. To overcome the identified crizotinib resistance, we performed high throughput drug screening, and found that the cMET/RET/VEGFR inhibitor cabozantinib (XL184) effectively inhibited the survival of both WT and crizotinib resistant mutated CD74-ROS1-expressing Ba/F3cells. Since cabozantinib (XL184) is clinically available for the treatment of thyroid cancer patient, the finding that cabozantinib can overcome the crizotinib resistances caused by secondary mutations in ROS1, potentially could change the therapeutic strategies for ROS1 rearranged NSCLC.

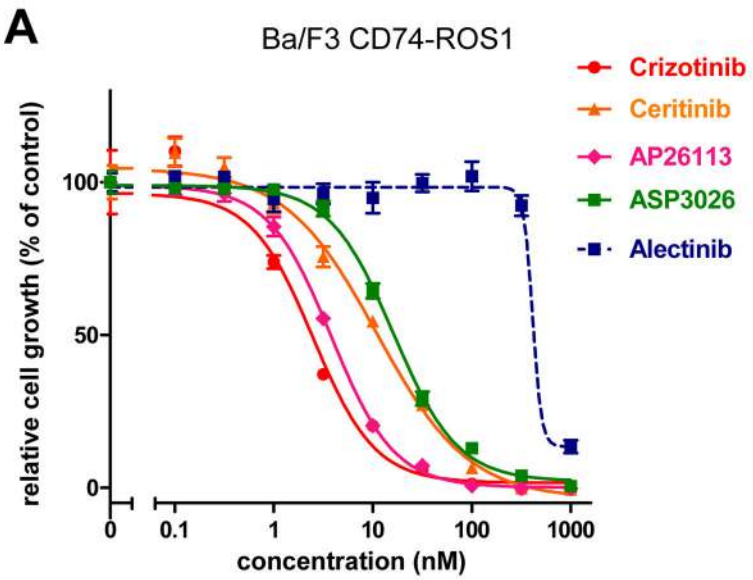

B

Drugs	IC_{50} (nM)
Crizotinib	2.12
Ceritinib	10.92
AP26113	2.68
ASP3026	16.11
Alectinib	586.6

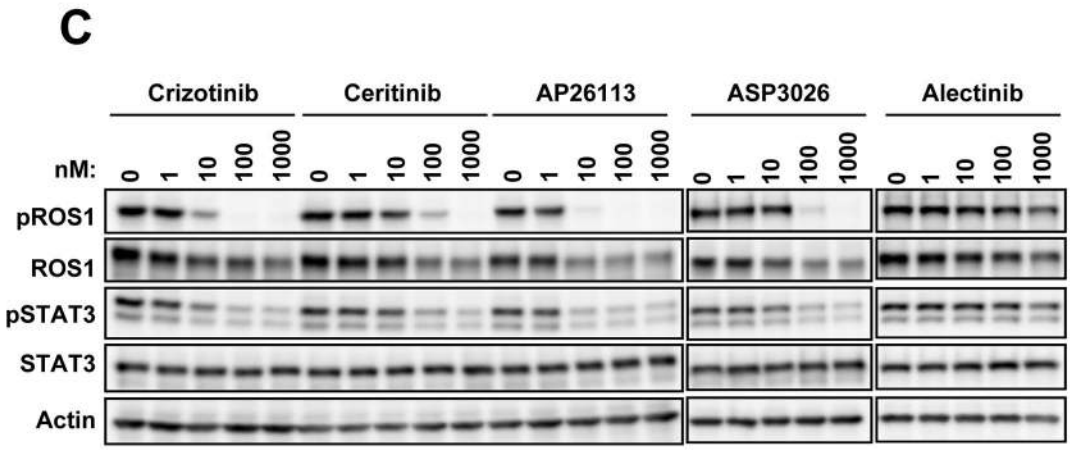

Figure 1. Several ALK inhibitors effectively inhibit the growth of CD74-ROS1-addicted Ba/F3 cells

(A) Ba/F3 cells expressing CD74-ROS1 (clone #6) were seeded in 96 well-plates and treated with indicated concentration of crizotinib, ceritinib, AP26113, ASP3026, or alectinib for 72 h. Cell viability was analyzed using the CellTiter-Glo assay. (B) IC_{50} values (nM) of Ba/F3 cell lines expressing CD74-ROS1 (clone #6) against various ALK inhibitors are shown. Average IC_{50} values against crizotinib, ceritinib or AP26113 were calculated from the 3 independent experiments. IC_{50} values against ASP3026 and alectinib were calculated from the single experiment. (C) Inhibition of phospho-ROS1 by various ALK inhibitors in Ba/F3 models. CD74-ROS1 expressing Ba/F3 cells were exposed to increasing concentrations of crizotinib, ceritinib, AP26113, or ASP3026 for 3 h. Cell lysates were immunoblotted to detect the indicated proteins.

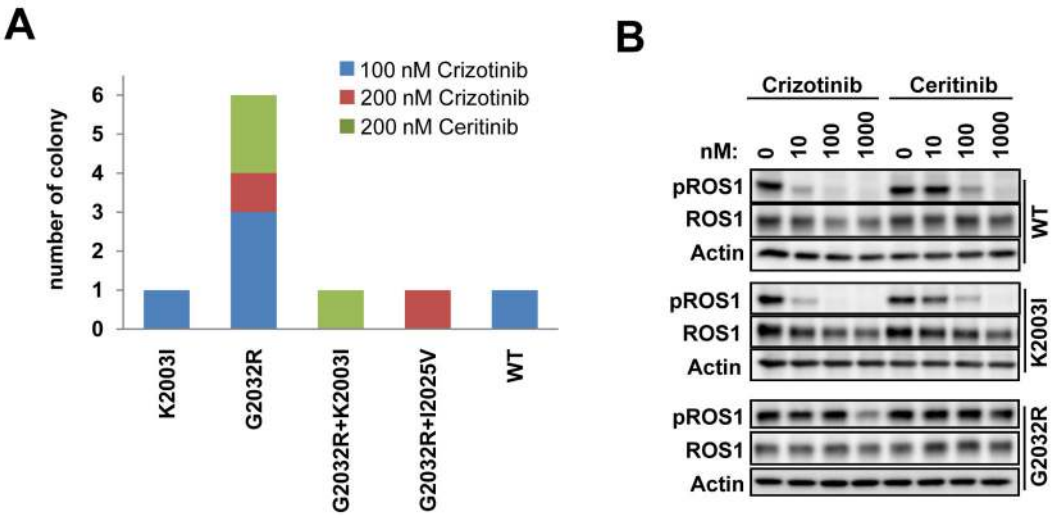

C

IC_{50} (nM)	Crizotinib	Ceritinib
WT	2.12	10.92
K2003I	1.52	11.69
G2032R	253.7	276.5
parental + IL-3	370.0	1163

Figure 2. Identification of crizotinib and ceritinib-resistant mutations by accelerated mutagenesis screening

(A) Number of the ROS1 kinase domain mutations found in the N-ethyl-N-nitrosourea (ENU)-treated CD74-ROS1 Ba/F3 clones isolated after growth in the presence of 100 and 200 nM of crizotinib or 200 nM of ceritinib. (B) Inhibition of phospho-ROS1 by crizotinib and ceritinib in ENU selected crizotinib- or ceritinib-resistant Ba/F3 clones. CD74-ROS1-wildtype expressing Ba/F3 cells clone 3 or ENU selected K2003I or Ba/F3 cells harboring the G2032R mutation were exposed to increasing concentrations of crizotinib or ceritinib for 2 h. Cell lysates were immunoblotted to detect the indicated proteins. (C) IC_{50} values for CD74-ROS1 kinase domain mutant Ba/F3 cells treated with crizotinib or ceritinib. IC_{50} values are shown in the lower table. IC_{50} values of Ba/F3 parental cells cultured with IL-3 and CD74-ROS1-WT expressing Ba/F3 cells were shown for comparison.

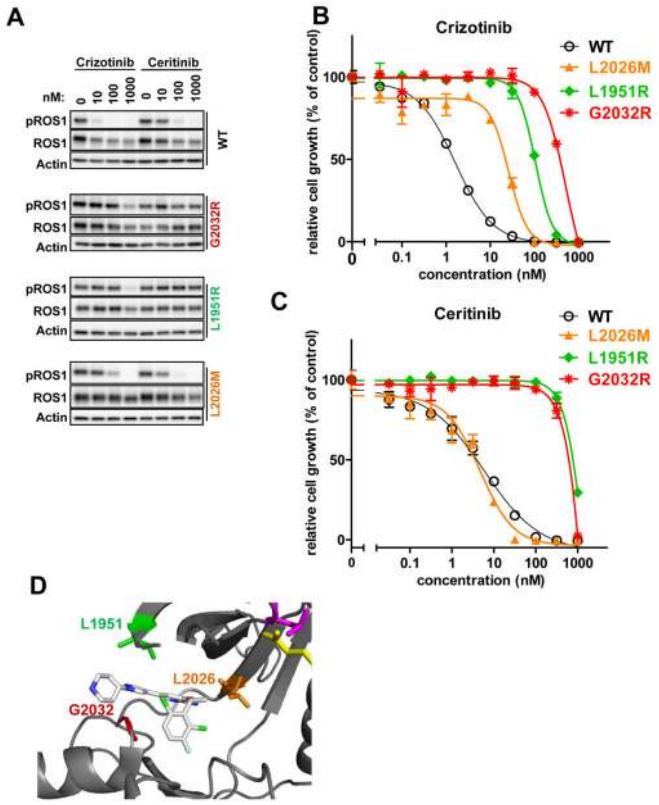

Figure 3. Sensitivity of the CD74-ROS1 mutant reintroduced Ba/F3 cells to crizotinib or ceritinib

(A) Inhibition of phospho-ROS1 by crizotinib and ceritinib in each WT or mutant CD74-ROS1 introduced Ba/F3 cells. Each Ba/F3 cells were exposed to increasing concentrations of crizotinib or ceritinib for 2 h. Cell lysates were immunoblotted to detect the indicated proteins. (B, C) WT or mutant (G2032R, L1951R, or L2026M) CD74-ROS1-introduced Ba/F3 cells were seeded on 96-well plates and treated with the indicated concentration of crizotinib (B) or ceritinib (C) for 72 h. Cell viability was analyzed using the CellTiter-Glo assay. IC-50 values of each mutant Ba/F3 clone to crizotinib or ceritinib were shown in Supplementary Figure S4B. (D) Resistant mutation residues in the structural models of wild-type ROS1 kinase domain with crizotinib. Three-dimensional mapping of each identified ROS1 mutation based on the crystal structure of ROS1 with crizotinib. Each of the three ROS1 mutations is mapped on a ribbon diagram. Figures were drawn using PyMol software with the crystal structure information of PDB ID 3ZBF. Other identified mutations mapped on the whole ROS1 kinase domain is shown in Supplementary Figure S5.

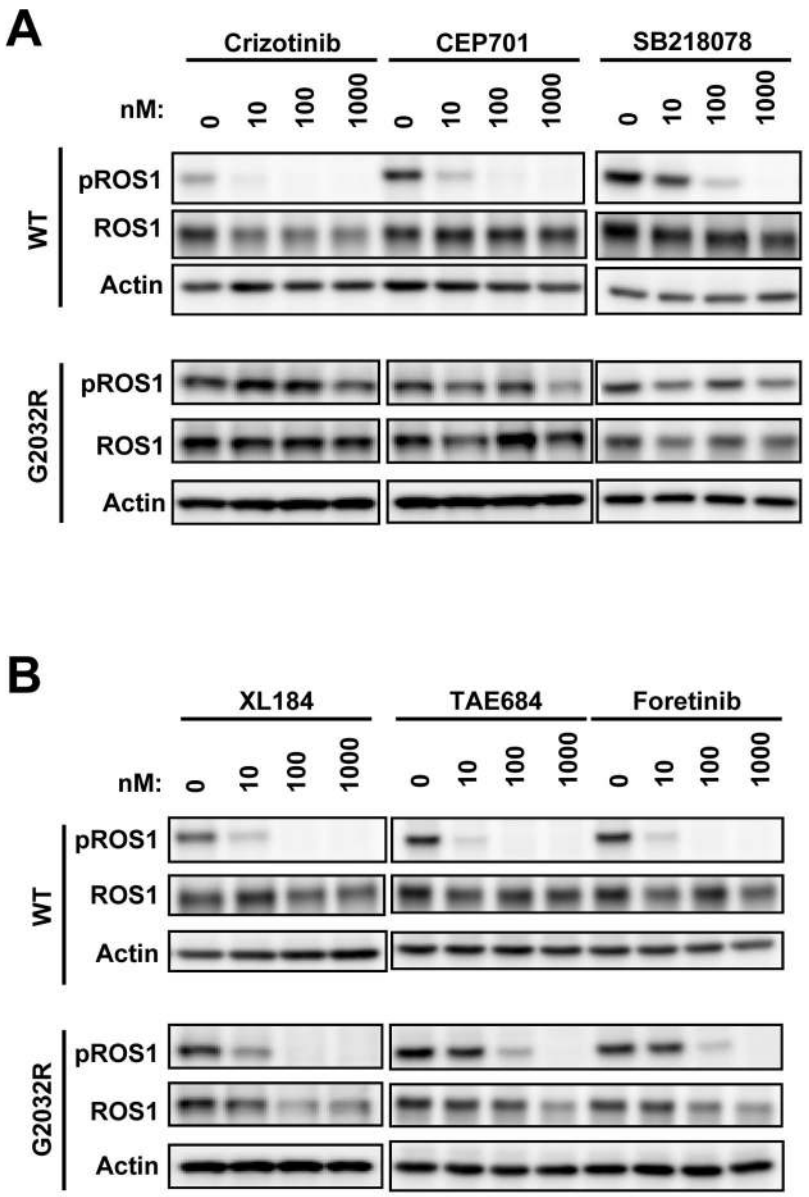

Figure 4. Newly identified inhibitors effectively inhibit phospho-ROS1 of wildtype CD74-ROS1, or both WT and G2032R crizotinib-resistant mutant

(A, B) Inhibition of phospho-ROS1 by various identified ROS1 inhibitors selected from the high throughput screening. CD74-ROS1-WT-expressing (clone 6) or CD74-ROS1-G2032R-expressing Ba/F3 cells were exposed to increasing concentrations of crizotinib, CEP701, SB218078 (A), cabozantinib (XL184), TAE684, or foretinib (B) for 2 h. Following treatment, the cell lysates were immunoblotted to detect the indicated proteins.

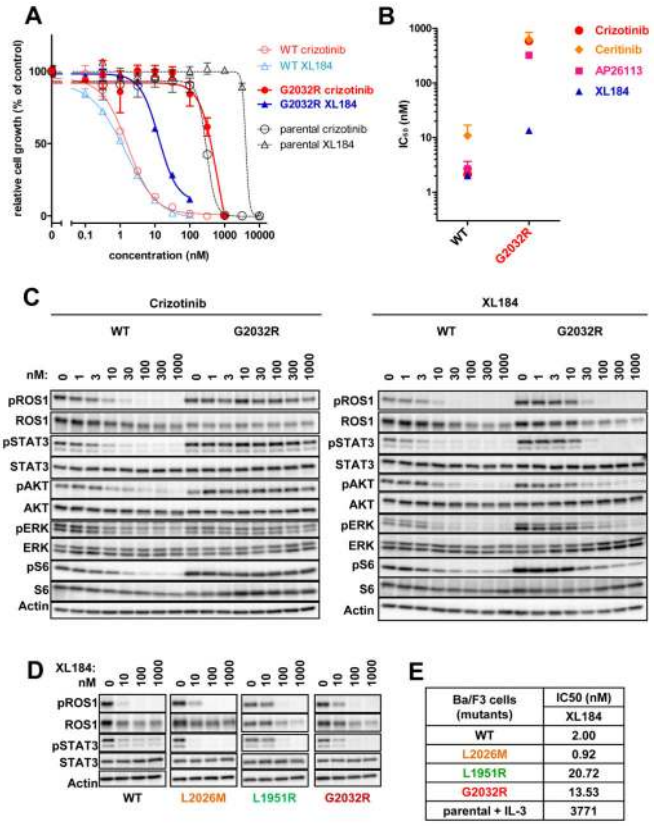

Ba/F3 cells (mutants)	IC50 (nM)
	XL184
WT	2.00
L2026M	0.92
L1951R	20.72
G2032R	13.53
parental + IL-3	3771

Figure 5. Cabozantinib overcomes crizotinib-resistance caused by the mutations in CD74-ROS1

(A) Ba/F3 parental cells (with IL-3) or those expressing CD74-ROS1-wildtype (WT) or CD74-ROS1-G2032R were seeded in 96-well plates and treated with the indicated concentration of crizotinib or cabozantinib (XL184) for 72 h. Cell viability was analyzed using the CellTiter-Glo assay. (B) IC_{50} values of Ba/F3 cells expressing WT or G2032R mutated CD74-ROS1 treated with crizotinib, ceritinib, AP26113 or cabozantinib (XL184). (C) Comparison of the inhibition of phospho-ROS1 and its downstream by crizotinib and cabozantinib in Ba/F3 cells expressing CD74-ROS1 WT or G2032R exposed to increasing concentrations of crizotinib or cabozantinib (XL-184) for 2 h. Cell lysates were immunoblotted to detect the indicated proteins. (D) Inhibition of phospho-ROS1 by cabozantinib in each mutant expressing Ba/F3 cells. CD74-ROS1 WT or mutants expressing Ba/F3 cells were exposed to increasing concentrations of cabozantinib for 2 h. Cell lysates were immunoblotted to detect the indicated proteins. (E) Average IC50 values (from the 3 independent experiments) of each Ba/F3 cells to cabozantinib (XL184) were shown.

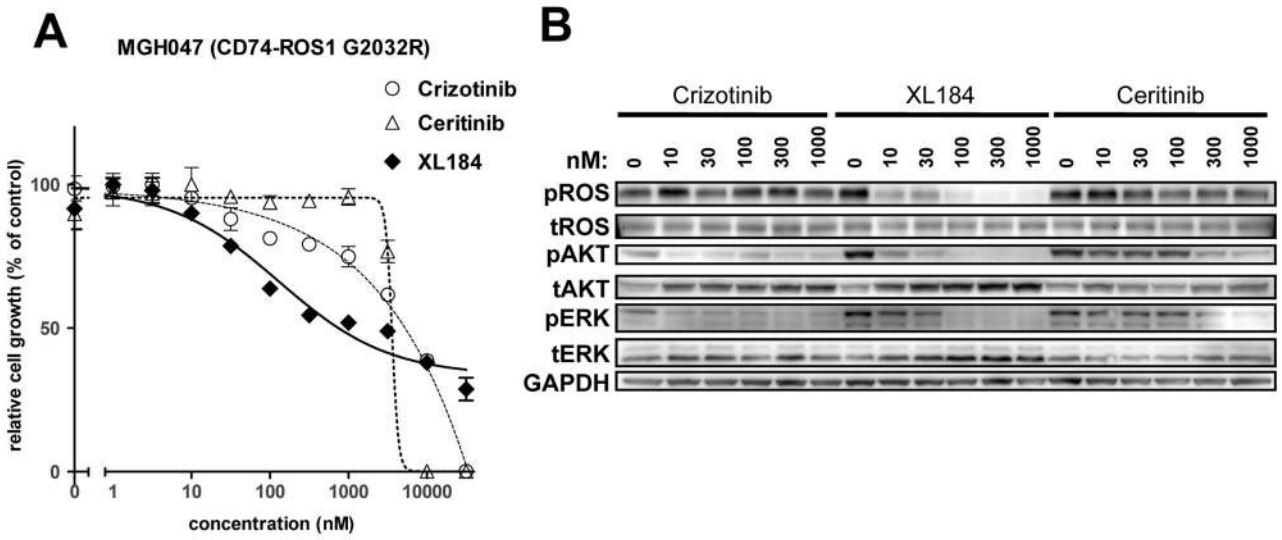

Figure 6. Cabozantinib inhibits the growth of G2032R mutation harboring MGH047 cells and the phosphorylation of CD74-ROS1

(A) Crizotinib-resistant CD74-ROS1-positive NSCLC patient-derived MGH047 cells were seeded on 96-well plates and treated with the indicated concentration of crizotinib ceritinib or and cabozantinib (XL184) for 7 days. Cell viability was analyzed using the CellTiter-Glo assay. (B) Comparison of the inhibition of phospho-ROS1 and its downstream signaling by crizotinib, cabozantinib or ceritinib in CD74-ROS1 G2032R expressing MGH047 cells. MGH047 cells were exposed to the indicated concentrations of crizotinib cabozantinib (XL184) or ceritinib for 6 h. Cell lysates were immunoblotted to detect the indicated proteins.

Table 1

Kinase inhibitor screening identified multiple inhibitors which is active against CD74-ROS1-Wildtype (WT) and G2032R crizotinib-resistant mutant

The top 9 list of inhibitors, which specifically inhibit the growth of CD74-ROS1 expressing Ba/F3 cells, obtained from high throughput screening of 282 inhibitors. Ba/F3 parental cells (with IL-3) or those expressing CD74-ROS1-WT or CD74-ROS1-G2032R were seeded in 96-well plates and treated with the indicated concentration of various inhibitors for 72 h. Cell viability was analyzed using the CellTiter-Glo assay. The average cell viability (% of control) of the top 9 inhibitors is shown. All of the screening data are shown in Supplementary Table S1.

	parental BaF3 (+IL-3)				**CD74-ROS1 (WT)**				**CD74-ROS1 (G2032R)**			
	3 μM	**1 μM**	**100 nM**	**10 nM**	**3 μM**	**1 μM**	**100 nM**	**10 nM**	**3 μM**	**1 μM**	**100 nM**	**10 nM**
AP26113	**2.4**	**16.6**	101.6	104.7	**0.2**	**0.5**	**1.5**	30.0	**0.4**	**1.2**	76.5	114.8
crizotinib	**2.5**	**5.2**	102.7	106.0	**1.4**	**1.9**	**4.4**	42.0	**2.7**	**2.3**	109.8	120.2
ceritinib	**1.3**	74.8	104.6	103.0	**0.6**	**0.8**	**5.2**	62.1	**1.1**	**9.7**	102.2	109.3
ASP3026	69.4	96.3	110.7	100.9	**0.3**	**0.8**	**8.5**	74.9	**6.0**	58.8	101.0	110.0
SB218078	**4.1**	**5.9**	41.8	104.7	**1.3**	**1.9**	**1.9**	40.0	**2.2**	**3.1**	**28.9**	96.4
CEP701	**1.6**	**2.5**	47.3	96.6	**1.5**	**1.2**	**1.4**	32.5	**1.4**	**1.6**	**12.9**	97.0
TAE684	**1.6**	**8.9**	99.4	102.6	**0.3**	**0.5**	**0.9**	**10.7**	**0.5**	**0.5**	**10.1**	110.2
XL184	77.1	105.7	111.2	101.1	**0.3**	**1.0**	**1.1**	**21.2**	**0.5**	**0.6**	**5.6**	90.4
Foretinib	**3.3**	**2.8**	94.0	108.5	**0.5**	**0.7**	**1.7**	32.3	**0.7**	**0.7**	**14.9**	110.9

Each number indicates cell viability (% of vehicle treated control)

Clin Cancer Res. Author manuscript; available in PMC 2016 January 01.